Chapter 7
The Climate System

Gordon M. Heisler and Anthony J. Brazel

Abstract Interesting but sometimes complex interacting processes cause differences in climate between more urbanized areas and nearby less urbanized areas. This chapter aims to provide an understanding of urban climate systems and the ecological significance of the differences between rural and urban climate. We include explanations of terms, units of measurement, and basic equations that are commonly used in the expanding scientific literature from urban climate research around the world. We describe the physical processes that govern energy balances of urban landscapes—human-caused heat input; modified solar and thermal radiation; transfer of sensible heat, which we feel as air temperature differences; and movement of heat by evaporation and condensation of water. The urban effects on energy transfer and the flow of air in the lower layers of the Earth's boundary layer cause temperature differences between urban and rural areas known at the urban heat island (UHI) effect, which can commonly reach intensities of 10 °C. This effect is a main focus of the chapter. UHIs are altered by topographic influences that sometimes overwhelm urban land cover influences on air temperature. We describe types of UHIs and provide examples, the methods used to detect UHIs, and the influences of tree cover and parks. We briefly describe the effects of urban structure on wind, including thermally driven flow. Finally, we relate urban climate to global climate change and explore some of the difficulty of separating urbanization influences from global climate change.

Keywords Heat island · Land cover · Parks · Urban boundary layers · Urban forests

---

Electronic supplementary material: The online version of this chapter (https://doi.org/10.1007/978-3-030-11259-2_7) contains supplementary material, which is available to authorized users.

G. M. Heisler (✉)
USDA Forest Service, Syracuse, NY, USA

A. J. Brazel
School of Geographical Sciences and Urban Planning, Arizona State University, Tempe, AZ, USA
e-mail: abrazel@asu.edu

M. H. P. Hall, S. B. Balogh (eds.), *Understanding Urban Ecology*,
https://doi.org/10.1007/978-3-030-11259-2_7

7.1 Introduction

The goal of this chapter is to describe climatic conditions and processes that are different in urban areas from those in other landscapes—agricultural, grass land, or forested. Urbanization modifies all of the variables that make up weather and climate—air temperature, humidity, wind, precipitation, cloud cover, and both thermal and solar electromagnetic radiation. Of these variables, the one that is generally most obvious and probably the most studied is the presence of temperatures that differ from those in nearby rural areas. Within cities, temperatures are generally, though not exclusively, warmer [1].

In contrast to global climate change, which is somewhat hard to detect because it has effects over large parts of the Earth over long time periods and is more difficult to measure, the influence of cities on temperature in and near them is relatively easy to determine. In the case of global climate change, it is somewhat difficult to determine whether change is caused entirely by human activity or partly by processes that would take place without people. The cause of urban influences on climate is obvious—human-built structures and activity—and these produce radically altered local environments [2]. In many cities, global environmental changes are swamped by dramatic changes in the local environment [3]. In this chapter we explore these changes, especially to temperatures, as background for discussion of broader urban ecology, which integrates natural and social sciences generally and in other chapters in this book. The ecological considerations are important because cities create both the problems and solutions to sustainability challenges in our increasingly urbanized world [2].

Generally increased temperature in cities compared to nonurban areas, termed the *urban heat island* (UHI) effect, is present in cities all around the world and contributes to global climate change in several ways. In turn, the effects of UHIs are increased by global climate change [4, 5]. In an energy-constrained future, the importance of urban temperatures will increase in many climates, because high temperatures lead to greater energy use for air conditioning. This is especially true in climates in which buildings can be cooled by opening windows to reduce reliance on air conditioning, because there will be fewer hours of cool outside air [6]. The UHI effect creates one of the key challenges to evaluating the influence of *greenhouse gases*[1] on global climate change, because urban influences are present in archived historical weather data that are used to determine long-term climate trends [7].

One goal of this chapter is to present some of the terminology that is commonly used in the scientific literature about urban climate. Both *meteorology*, the instantaneous or short-term processes in the atmosphere, and *climate*, the longer-term average, maximum, and minimum values of atmospheric features, may be described at a large range of spatial scales. Urban atmospheric processes are usually described at

[1] Carbon dioxide, methane, and other gases that are transported from sources near the ground into the upper atmosphere and act to intercept longwave radiation from the Earth's surface.

Table 7.1 Scales used in descriptions of atmospheric processes [8]

Scale name	Range of length	Typical area
Microscale	10^{-2} to 10^{3} m	Single family home patio to a city block
Local scale	10^{2} to 5×10^{4} m	Several city blocks to the size of a small city
Mesoscale	10^{4} to 2×10^{5} m	A large city to one or two states
Macroscale	10^{5} to 10^{8} m	Weather-map-sized areas, whole continents

the *microscale* or *local scale*, and sometimes at the *mesoscale*, where the overlapping horizontal ranges of the scales are given approximately as in Table 7.1. Weather forecasting is done with consideration of conditions at the *mesoscale* and *macroscale*, sometimes referred to as the *synoptic* scale.

Urban meteorological and climatic impacts include effects on human health and comfort, energy use for space conditioning of buildings, air pollution, water use, plant growth and other biological activity, ice and snow, precipitation and flooding, and even environmental justice. In this chapter we emphasize urban climatic influences and processes that affect the urban air temperatures. We especially consider those influences that are most likely to be modified by urban design or management. Examples include the amount and distribution of park land and other open space, tree and other vegetation within the open space, overall distribution of vegetation within developed portions of the city, the use of irrigation to maintain vegetation, and "urban whitening," changing the reflectivity of pavements or roof surfaces by reflective paint or construction with reflective materials.

In following sections, the basic energy transfer processes of any landscape are described—radiation, sensible and latent flux,[2] and storage in soil and vegetation. This leads to the notation used to describe landscape energy budgets. With the energy budget concept in mind, the following sections consider urban influences on the energy budget, urban influences on the atmospheric boundary layer, and urban interactions with topographic influences including water bodies. Then we provide examples of urban heat islands, the methods used to detect them, and the influences of tree cover and parks. We briefly describe the effects of urban structure on wind, including thermally driven flow. The important concerns related to urban influences on meteorology and climate come next—human comfort and health, energy use in buildings, and precipitation. Finally, we relate urban climate to global climate change and explore some of the difficulty of separating urbanization influences from global climate change.

[2] A "flux" is the transfer of some quantity, such as an amount of energy, per unit time. Energy may be measured in joules (J), and 1 J per second, J s^{-1}, is 1 W. Thus, the unit watt (W) is a flux. Flux density is flux per unit area, such as the number of watts through an area of 1 m^2, W m^{-1}.

7.2 Physical Processes in Climate Systems

7.2.1 Radiant Energy Exchange

The energy that causes what we call climate begins with the sun. The sun's energy comes to Earth as *electromagnetic radiation*.[3] All objects give off electromagnetic radiation, which can be conceptualized as having waves with a peak-to-peak length that depends upon the temperature of the object's surface. The temperature at the surface of the sun is about 6000°K,[4] and the electromagnetic radiation from the sun that gets through Earth's atmosphere has a peak within the human visible range of wavelengths, which is about 400–700 nanometers[5] (nm). The total range of the solar spectrum on Earth is from 280 nm to about 3000 nm (or 0.28 micrometers, abbreviated μm, to 3 μm), and we call this whole range *shortwave* or *solar* radiation.

Surfaces with temperatures near those we commonly encounter around us in cities, about 300°K, emit radiation in the spectrum from about 4 to 30 μm. We call this *longwave* or thermal radiation. The intensity of radiation per μm and per unit area is about 10,000,000 times greater in shortwave (*S*) than longwave (*LW*) radiation. When incoming shortwave radiation, $S_{\downarrow}$, strikes an object, it may be either absorbed or reflected. The fraction of $S_{\downarrow}$ reflected is called the *albedo* of that surface, often abbreviated by α. In mathematical form, absorbed shortwave radiation is given by

$$S_{\text{abs}} = \left(1-\alpha\right)S_{\downarrow} \tag{7.1}$$

Generally, the lighter the color is, the higher the albedo. The urban whitening method proposed for cooling cities uses paint or special roofing or paving materials to increase α of the city, so that S_{abs} is lower and less shortwave radiation is available to heat the city [9].

The rate of radiation emitted by a surface depends upon the temperature of the surface and a characteristic of the material, the *emissivity*, ε, which is the amount of radiation emitted relative to the amount that would be emitted by a black body[6] for a given temperature. Most materials in nature have an ε of about 0.95. The governing equation for emitted longwave radiation is

$$\text{LW} = \sigma\varepsilon T_K^4 \tag{7.2}$$

[3] Electromagnetic radiation is energy transfer through space by disturbances in electric and magnetic fields that can be described as waves that have different wavelengths of oscillation in a continuous spectrum.

[4] In the Kelvin scale of temperature, 0 °K is absolute 0 and it is identical to −273.15 °C.

[5] In meteorology and climatology, the spectrum of solar electromagnetic radiation is commonly measured in nanometers, 1 nm = 0.000000001 m (1×10^{-9} m). The spectrum of thermal radiation is commonly measured in μm, 1 μm = 0.000001 m (1×10^{-6} m).

[6] A black body is a conceptual opaque and non-reflective object that is perfectly absorbing longwave radiation and emits at the same rate.

where σ is a constant, called the *Stefan-Boltzmann constant* and T_K is Kelvin temperature of the surface. Thus, longwave radiation from the sky toward the ground, $LW_{\downarrow}$, is $\sigma\varepsilon_a T_K^4$, where ε_a is atmospheric emissivity. Longwave radiation from the ground surface, $LW_{\uparrow}$, is $\sigma\varepsilon_e T_K^4$, where ε_e is emissivity of the Earth or ground surface. The ε of a surface also governs its absorbance of incoming longwave radiation.

We now have the components that make up an important part of the explanation of climate of a city, or any other area—the net radiation, Q^*, the total short and longwave radiation absorbed by the Earth surface, which in equation form is

$$Q^* = S_{\text{abs}} + \text{LW}_{\downarrow} - \text{LW}_{\uparrow}. \tag{7.3}$$

The symbol Q with a superscript or subscript letter or symbol is commonly used to represent a heat flux in energy budget equations.

On cloudy nights, T_K of the sky and ground surface are similar, so that $LW_{\downarrow}$ and $LW_{\uparrow}$ are nearly equal. However, on cloud-free nights, the effective T_K of the sky may be much less than T_K of the ground surface, so that rapid cooling of the surface results.

7.2.2 Heat Flow

Heat flows into and from air in two forms. When air absorbs or gives up heat and air temperature increases or decreases, the amount of heat is termed *sensible heat*, heat you can feel. If liquid water evaporates to become vapor in air, energy is required to evaporate the water, and that energy is termed the *latent heat of vaporization*. This heat energy is contained within the vapor. The reason it is called "latent" (potential but not evident) is that when air is cooled below a certain temperature, which depends on the amount of vapor in the air, vapor condenses and gives up the latent heat. The lower the temperature at which condensation begins (*dew point temperature*), the drier the air. The latent heat of vaporization, about 2.5 MJ/kg of water evaporated, is a major factor in determining climate, because it uses energy from Q^*. The more Q^* is used in latent heat production, the less Q^* is available for sensible heat creation. Latent heat production has the potential to consume a large amount of Q^*. It takes nearly six times more energy to evaporate 1 kg of water than it takes to heat 1 kg of liquid water from 0 °C all the way to 100 °C.

When the surface temperature changes, energy flows into and out of soil, rock, plant material, or human-made objects like roads and buildings in response to temperature differences between the surface and the interior of the substance. This is termed heat *storage*. For a given temperature difference, the rate of flow depends upon the thermal properties of the material (Table 7.2). *Density* is simply mass, the amount of "stuff," per unit of volume, and though density affects the thermal properties, it is not itself considered one of the thermal properties. *Thermal conductivity* is the ability to conduct heat, the quantity of heat (in units of joules, J) flowing through a cross sectional area (m^2) each second (s) if there is a temperature gradient

Table 7.2 Thermal properties of typical urban interface materials [8]

		Specific	Heat	Thermal	Thermal
	Density[a]	Heat, c	Capacity, C	Conductivity, k	Admittance, μ
Material	Kg $m^{-3} \times 10^3$	J kg^{-1} $K^{-1} \times 10^3$	J m^{-3} $K^{-1} \times 10^6$	W m^{-1} K^{-1}	J m^{-2} K^{-1} $s^{-1/2}$
Urban materials					
Asphalt	2.11	0.92	1.94	0.75	1205
Brick	1.83	0.75	1.37	0.83	1065
Concrete	2.40	0.88	2.11	1.51	1785
Glass	2.48	0.67	1.66	0.74	1110
Steel	7.85	0.50	3.93	53.3	14,475
Natural materials					
Air (20 °C)	0.0012	1.01	0.0012	0.025	5
Sand (dry)	1.60	0.80	1.28	0.30	620
Soil (dry clay)	1.60	0.89	1.42	0.25	600
Soil (wet clay)	2.00	1.55	3.10	1.58	2210
Water (20 °C)	1.00	4.18	4.18	0.57	1545
Wood, light	0.32	1.42	0.45	0.09	200

[a]The values for density, specific heat, and heat capacity are scaled by the exponents of 10 to keep them to an easily handled size in the table. For example, for asphalt the density is 2110 kg/m^3, and heat capacity is 1,940,000 J/m^3 for each 1 °K of temperature change

(1° K m^{-1}, or 1-degree Kelvin per meter) perpendicular to the area. The units J s^{-1} (joules per second) are equivalent to 1 watt (W), so the units given in Table 7.2 for thermal conductivity are W m^{-1} K^{-1}. The temperature change (K^{-1}) in a given mass of a material for a given amount of heat absorbed (J) depends upon the *specific heat*, c, with units of J kg^{-1} K^{-1} when considering the heat required for a unit of mass (kg) or when considering heat required per unit volume, the *heat capacity*, C, with units of (J m^{-3} K^{-1}).

Thermal admittance, μ, of a surface is especially interesting for urban climate because it determines the amount of heat (J) that will pass from the surface into the material for a given heat source. Though the units are somewhat difficult to grasp intuitively, the effects of μ are easy to feel. For example, nearly everyone has the experience of feeling the hot sand when walking barefoot across a beach of dry sand. Dry sand has low thermal admittance, and it gets very warm because little of the absorbed heat from the sun is carried into lower layers of the sand. Another intuitive appreciation of thermal admittance comes from touching two materials—one of steel the other of wood—with the same temperature, say 20 °C, room temperature in a building. Because of its extremely high thermal conductivity, the steel has high μ (see Table 7.2) and will feel cool because it rapidly removes heat from your finger, which is at skin temperature of about 30 °C, whereas wood, with low μ, will transmit little heat from your finger and feel relatively warm to the touch [8]. Materials with high admittance tend to store large amounts of heat during the day and release it at night—one of the effects that makes urban areas warmer than rural. Thermal admittance is proportional to conductivity and heat capacity. It can be

calculated from columns 4 and 5 in Table 7.2 as $(k \times C)^{1/2}$. Note in Table 7.2 that most urban materials (except for wood, which could also be considered an urban material) have high μ compared to the natural materials, except for water and wet soil.

An implication for urban design is that night-time cooling will be enhanced if the surface is covered by low-admittance materials. However, if low-admittance surface materials cannot be used, greater cooling will occur if sky view (the percent of sky visible above a point on the ground) is greater, for example, with wider spacing between buildings. Cooling increases with increase in sky view unless μ is very low [10].

7.2.3 Energy Budget Concept

The *energy budget* for an area on Earth is largely responsible for temperature differences between that area and other areas with different energy budgets. Symbolically, the energy budget for a surface, such as flat bare soil is

$$Q^* = Q_E + Q_H + Q_G \tag{7.4}$$

Here, Q^* is net radiation as in Eq. 7.3, Q_E is the flux of latent heat (latent heat of vaporization, see Sect. 7.2.2), Q_H is sensible heat flux, and Q_G is storage of heat in the soil. In most landscapes, Q_E results from evaporation from water bodies and soil or transpiration from plants, and we call the combined process *evapotranspiration*.

The energy budget concept may be applied to other surfaces—one side of a single tree leaf [11], the skin of a person [12], or the wall of a building [8]. Energy budgets may also be calculated for the upper surface of an agricultural crop, a forest, or a city, but, while the general level of the tops of trees or buildings may be considered to be a surface, there is actually a volume below that surface that contains the trees or buildings, and that volume may be visualized as an imaginary box [8]. Then the storage term, often designated as ΔQ_S, must include the heat storage within those trees or buildings in the volume in addition to the soil storage Q_G [13]. Another complication for the energy budget of such a volume, or "box," is that air can move into the box from the side, a process termed *advection*. Advection is usually assumed to be small relative to Q^*, an assumption generally necessitated by the difficulty of measuring advection.

7.3 The Urban Energy Budget

Urban influences on temperature differ from rural areas because of differences in their energy budgets. These energy budget differences are caused in part by differences in the properties of materials found in rural and urban areas. The different

materials cause differences in total heat storage, ΔQ_S, which includes heat storage in aboveground objects as well as storage in the soil, Q_G. Another difference is that urban energy budgets have an additional component—human-produced heat sources or *anthropogenic* heat emissions, Q_F—that must be added to net radiation as a heat input [14]. With the new terms, the urban energy budget becomes:

$$Q^* + Q_F = Q_E + Q_H + \Delta Q_S \tag{7.5}$$

7.3.1 Anthropogenic Heat Sources

The methodology to evaluate the different sources of anthropogenic heat, Q_F in Eq. 7.5, in an urban energy budget is challenging but interesting [14]. Combustion heat has been estimated for some cities by analysis of consumer usage of fuel such as gas and electricity considering, for example, the number of vehicles, distance traveled, and fuel efficiency. Total anthropogenic emissions range from nil to 300% of net radiation, depending upon the amount of industrialization. Generally, Q_F is higher in more industrialized cities, in high-latitude cities, and in winter. It is composed primarily of heat produced by combustion of vehicle fuels, from heating and cooling buildings, and heat released from industrial processes. Even metabolism in human bodies can be a heat source, though it is generally <1% of total Q_F and can be ignored. There is a positive feedback loop between air conditioning and urban warming. As a city becomes warmer, increased use of air conditioning adds significantly to additional warming [14].

A mesoscale modeling study (see Sect. 7.6.5) of Philadelphia, PA, gives an idea of the importance of Q_F in urban energy budgets [15]. Summer anthropogenic heating ranged from about 20 W m^{-2} at night to around 50 W m^{-2} during the day. This compares with typical peak daytime solar radiation of around 700 W m^{-2}. During the day, Q_F had a negligible effect on air temperature, but it increased temperature about 0.8 °C at night. In winter the anthropogenic heating ranged from about 35 W m^{-2} at night to around 85 W m^{-2} during the day. The peak daytime solar radiation levels in winter were only about 460 W m^{-2}, much less than in summer. The Q_F heating in urban temperature simulations increased air temperature by 0.5–0.8 °C during the winter day and 2–3 °C during the winter night.

7.3.2 The Urban Radiation Balance

An urban area affects the exchanges of shortwave and longwave radiation by increased air pollution and by complex changes of surface radiative characteristics. The atmospheric attenuation (reduction of radiation by scattering and absorption) of incoming shortwave radiation by pollution has been analyzed in numerous urban

environments. The attenuation in the atmosphere over cities is typically 2–10% more than in the surrounding rural areas. Generally, the very shortest wavelengths (<0.4 μm) of the electromagnetic spectrum to reach the surface of the Earth, the *ultraviolet* or *UVB* portion, are commonly depleted by 50% or more [16]. However, total depletion across all solar wavelengths (0.15–4.0 μm) is <10%. The processes of scattering and absorption are greatly modified by the urban aerosol characteristics and concentrations [17].

Another effect of urbanization is the change in albedo, which is typically slightly less in urban areas than in the surrounding landscape. Lower albedo is due in part to darker surface materials making up the urban mosaic and also to the effects of trapping shortwave radiation by the vertical walls and the urban, canyon-like morphology. There is considerable variation of albedo within the city depending on the vegetative cover, building materials, roof composition, and land use characteristics. The difference in albedo between a city and its surrounding environment also depends on the surrounding terrain. A city and a dense forest may differ a little in albedo; both may range from 10% to 20%. Urban trees lead to cooler cities because they store little heat and cool by evapotranspiration, not by having high albedo. In winter, a mid-latitude to high-latitude city with surrounding snow cover may display a much lower albedo than its surroundings. Thus, since cities receive 2–10% less shortwave radiation than their surroundings yet have slightly lower albedo (by <10%), most cities experience very small overall differences in absorbed shortwave radiation relative to rural surroundings [18].

Longwave radiation is affected by city pollution and the warmer urban surfaces. Warmer surfaces promote greater thermal emission of energy vertically upward from the city surface compared to rural areas, especially at night. Some longwave radiation is reradiated by urban aerosols back to the surface and also from the warmer urban air layer. Thus, increases in incoming longwave radiation and outgoing longwave radiation are usually experienced in urban areas. Outgoing longwave radiation increases are slightly greater than the incoming increases in the city, again especially on clear, calm nights. During daytime there is little difference between the city and its surroundings. Viewed from above a city, the overall surface emissivity can be different between country and city areas, and this may account for longwave radiation differences between urban and rural [19]. However, because a city structure is three-dimensional and variable, general statements about the overall urban versus rural emissivity and resulting effect on surface temperature of most cities cannot be made with confidence [20].

Longwave emission from soils and soil heat capacity are determined by soil moisture and hence by recent precipitation. Therefore, soil temperatures, and indirectly, air temperatures, depend upon precipitation [21, 22]. In a Baltimore study, air temperatures in rural landscapes became closer to urban air temperatures (smaller UHI) when recent precipitation was high.

7.3.3 Urban Sensible and Latent Heat Fluxes and Heat Storage

The partitioning of energy in urban areas among sensible (Q_H), latent (Q_E), and storage of heat (ΔQ_S and Q_G) primarily depends on the variety of land uses in the city compared to rural areas. Generally, the drier urban building and road materials induce higher Q_H, less Q_E, and higher ΔQ_S and Q_G in urban areas, all of which contribute to the UHI effect. However significant Q_E release does occur in many cities, because tree cover can be substantial, depending in part upon the general climatic region, with desert areas usually having lower tree cover (see Chap. 8). States in New England have average state-wide tree cover in their communities of 52–67%. Tree cover over some large cities such as Jersey City and San Francisco is about 12%, while Atlanta has about 37% tree cover. Especially in drier climates, Q_E is enhanced by irrigation [23, 24].

The value of Q_G and soil temperatures are greatly modified if asphalt covers the ground. In the soil of 2.5 m by 2.5 m tree planter boxes cut into the asphalt of a parking lot in New Brunswick, New Jersey, temperatures were compared to those in control planter boxes off the lot surrounded by grass instead of asphalt [25]. Near the center of the planter spaces on the parking lot, at a depth of 15 cm and 85 cm from the edge of the asphalt, maximum temperature exceeded controls by up to 3 °C. At the same depth but below the asphalt, maximum temperatures exceeded controls by up to 10 °C. Asphalt covering the soil not only increased maximum temperatures through a 60 cm profile but increased the rate of heat exchange since temperatures in the covered soil rose and fell more rapidly than control temperatures. In New Jersey, temperatures below the asphalt ranged from 0.5 to 34.2 °C, which was well within the toleration of tree roots. In contrast, temperatures below the asphalt of a parking lot in the warmer climate of Phoenix reached the likely plant-damaging temperature of 40 °C at a depth of 30 cm [26].

7.3.4 Energy Budget Examples

Measurements of above-canopy energy fluxes in Basel, Switzerland, over 30 days in midsummer (Fig. 7.1) illustrate the daily course of energy budgets at an urban, a suburban, and a rural location. Figure 7.1 uses the common convention that net fluxes toward the surface are positive, and fluxes away from the surface are negative. The net radiation, Q^*, is negative at night, meaning the net flux is upward, because $LW_{\uparrow}$ is greater than $LW_{\downarrow}$. Note the following: (1) in midday, the negative ΔQ_S means that heat is going away from the surface into storage, and positive ΔQ_S at night means heat is coming from storage toward the surface; (2) the magnitude of storage decreases from urban to rural; (3) sensible heat flux, Q_H, which is always negative, upward, is largest (most negative) in urban during the day and decreases in magnitude from urban to rural; and (4) latent heat flux (evaporation), Q_E, increases from

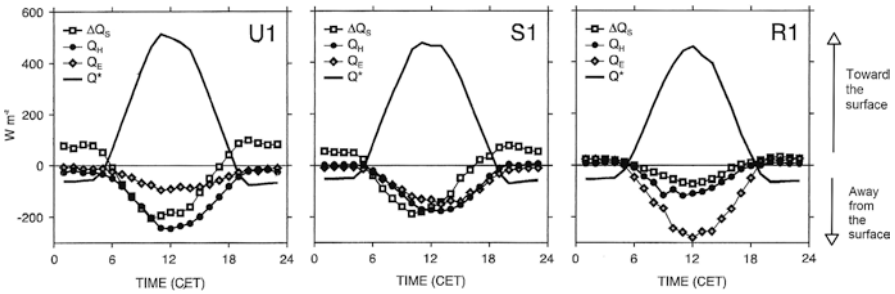

Fig. 7.1 Thirty-day average energy budgets for an urban site (U1), a suburban site (S1), and a rural site (R1) in or near Basel, Switzerland [27]

urban to rural. The partitioning of the net radiation, Q^*, into greater storage, greater sensible heat, and less latent heat in the more urbanized land uses explains the UHI effect.

7.4 The Urban Boundary Layer

7.4.1 Structure and Dynamics

The next step to understanding urban climate is to consider the structure of the Earth's boundary layer in urban areas, or UBL. The UBL is a modification by cities to the *planetary boundary layer* (*PBL*), also known as the *atmospheric boundary layer* (*ABL*) as diagrammed in Fig. 7.2. The PBL is the lowest part of the atmosphere that is directly influenced by its contact with the Earth's surface. The PBL depth, which varies from about 100–3000 m, is controlled by the surface roughness, temperature, moisture, and injections of pollutants. Solar heating of the surface during the day creates buoyancy of air in touch with it, and the resulting turbulent mixing expands the PBL toward its maximum depth. At night, cooling at the surface by outgoing longwave radiation causes the air flow to become smooth and nonturbulent, and the PBL shrinks to a depth of as little as 100 m [29]. Note that in the conceptual city of Fig. 7.2, which has a sharp rural to urban boundary, the UBL increases in thickness beginning at the upwind edge, and the UBL extends some distance downwind in a plume.

The UBL is divided into several layers by structural and dynamical features. For decades, urban climatologists have used an analogy with rural forests to describe urban structure in terms of the urban canopy layer (UCL), the space generally below the tops of trees and buildings. In humid-climate forests, the active surface, where most of the exchange of radiant energy and turbulent transport of water vapor and heat takes place, is usually a layer from the tops of trees down to the point where tree crowns meet. Foresters think of the forest canopy layer as the space between the tops of tallest trees and the bottom of tree crowns that bear living foliage. The active

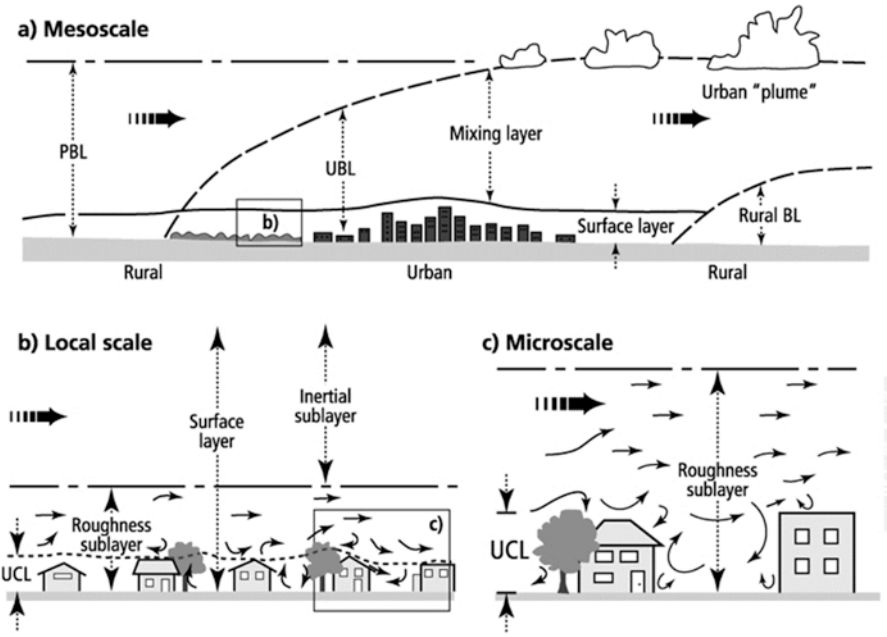

Fig. 7.2 Schematic of an urban boundary layer, UBL, within the planetary boundary layer (PBL). UBL sublayers and the (**a**) meso, (**b**) local, and (**c**) micro of Table 7.1 are also shown. From [28]

surface in urban areas is more variable than in closed natural forests, and the urban canopy layer is usually considered to be the entire space from the tops of trees or buildings, depending upon which dominates, down to ground level.

Within the roughness sublayer (Figs. 7.2 and 7.3), trees and buildings are dominant in creating the structure of turbulent wind flow and energy exchange; here eddies around individual buildings or trees (roughness elements) would be in evidence to sensors placed there. Above the RSL is the inertial sublayer where the influences of individual roughness elements have blended together so that although the friction with those elements is still present in affecting mean wind speed and the turbulent structure of the atmosphere, the effect of individual elements is no longer apparent. The RSL and the inertial sublayer together make up the surface layer where wind speed and turbulence, temperature, and humidity fluctuate greatly. Above the surface layer, these variables are nearly uniform with height.

The buoyancy and resulting amount of mixing within the PBL sublayer greatly influence the vertical air temperature profile and the hour to hour magnitude of UHI's. The buoyancy and mixing are described in terms of atmospheric stability. Mixing is strong during days with clear skies and light regional wind speed, and under these conditions, we say the PBL is *unstable*. During the night, if the sky is clear, radiative cooling lowers the temperature of the surface, the air just above the surface tends toward slow laminar flow, and the atmosphere is *stable*. With overcast sky or strong regional winds, or especially when both are present, temperature

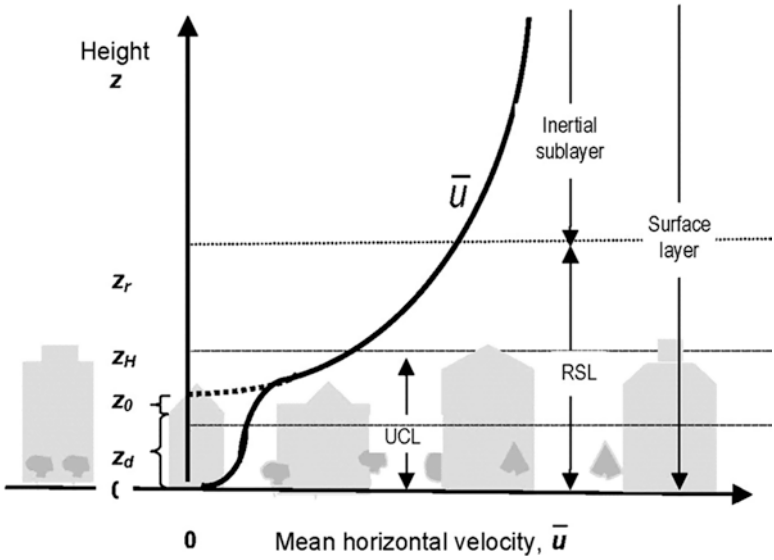

Fig. 7.3 Sublayers within the Earth's atmospheric surface layer in an urban area and a generalized mean vertical wind velocity ($\bar{u}$) profile. The measures on the height scale are the mean height of the roughness elements (z_H); the roughness sublayer (z_r and RSL); the zero-plane displacement (z_d) which is about 2/3 of z_H; and the roughness length (z_0), which is the height above z_d at which the above canopy wind profile extrapolates to 0 [30]

differs little with elevation, and we call this stability condition *neutral*. With strong wind speeds, there is much mixing of air in the surface layer, but it is mechanical, caused by turbulence from flow around trees and buildings, rather than thermal.

The mean horizontal wind speed, $\bar{u}$, within and above a relatively uniform UCL is depicted in Fig. 7.3. Starting near the top of the surface layer, $\bar{u}$ slows more and more as the top of the UCL is approached. The dotted line represents the extrapolation of the curve of wind speed, $\bar{u}$, to a theoretical zero near the top of the UCL at a height $z_o + z_d$. The roughness length, z_o, is aptly named because it defines the irregularity of a surface; z_o will be large for an urban area and very small for a relatively smooth surface such as a short agricultural crop. The shape of the $\bar{u}$ profile is influenced by the vertical motion contained in turbulent eddies generated by thermal and mechanical forces at the surface. These forces are carried upward on the eddies, which also mix the constituents of the atmosphere, including air pollutants, throughout the surface layer. The greater the turbulence-generating forces, the greater will be the mixing. Thus, mixing is greatest during unstable conditions and least under stable conditions.

Box 7.1: Indices of Atmospheric Stability
Atmospheric stability is critical not only to evaluating UHI effects but to evaluating dispersion of air pollutants. The state of this stability as it varies from

continued

Box 7.1 (continued)
day to night and with cloudiness and regional wind speed may be described by indices calculated from airport wind and cloud observations and elevation of the sun. One such index, the Turner Class, ranges from 1 for extremely unstable (little cloud cover, low wind speed near midday), to 4 for neutral (overcast sky or at least moderate wind speed or both), to 7 for very stable (clear sky, light wind at night) with values of 2, 3, 5, and 6 for intermediate conditions [21, 31].

Turner Class index has been shown to be a useful indicator of urban heat island intensity [21]. The conditions for a very stable atmosphere are also conditions that promote large UHI intensity. In Baltimore, MD, temperature differences between the city center and less developed points were usually larger with strong stability at night (Turner Classes 6 and 7)—see Sect. 7.6.4.

7.4.2 Topographic Influences on Urban Climate

Many cities are located in regions of considerable topographic variability. The terrain causes differences in local heating and cooling from place to place due to slope and exposure. Generally, heating of slopes and upper portions of valleys early in the day promotes local upslope and upvalley flow of warmer air, while after sundown a cooling of upper slopes and upvalley locales develops the impetus for downslope and downvalley cool air flow at night. Under relatively clear, calm weather, this local heating and cooling promotes thermally driven winds that vary in magnitude and direction during a diurnal period, much like a sea breeze system. Topographically generated air movement may have a large influence on temperature distribution, even in the small-scale topographic features of the East. Under stable atmospheric conditions (especially Turner Class 7, see Box 7.1), the relatively cool, heavy air near the ground moves by gravity downhill from higher elevations toward lower elevations. In some cities, this leads to effects on air temperature that may exceed the effects of land cover differences [21, 32, 33].

7.4.3 Measurements of Atmospheric Variables in Urban Areas

Routine air temperature measurements are often inaccurate because radiation, especially solar radiation, may cause large errors. In measurements for research and forecasting, temperature sensors are nearly always protected by shields to protect the sensors from radiation. However, unless the shields are aspirated by a fan, there will be significant errors during periods of full sun, sometimes of up to 5 °C or even more—errors that are significant in evaluating urban influences.

A cause of confusion about temperature differences is in the location of weather stations relative to ground cover and nearby obstacles. When the objective is to capture local scale or larger climate differences, temperature sensors should not be located close to buildings or near impervious ground cover, as is often done [34]. Confusion also results from station relocation, such as happened in Baltimore, Maryland, when the main city National Weather Service station was moved in May 1999 from the roof of a four-story building to a lawn near the water of the Inner Harbor. Loss of information about long-term temperature trends also results when stations are discontinued, such as happened to the Woodstock, Maryland, cooperative station, which was maintained for nearly a century until the 1990s.

To gain understanding of processes that create climate differences in urban areas, energy budget flux densities (as shown in Fig. 7.1) are often observed from tall towers (Box 7.2). Similar methods are used to measure fluxes of carbon dioxide (CO_2) to and from urban areas. Human-caused CO_2 emissions come from traffic, industrial processes, and heating and cooling of buildings. These sources of CO_2 are a concern for their contributions to global climate change.

Box 7.2: Measurements from Tall Towers

Observations of urban energy budget flux densities from tall towers generally use the *eddy correlation* (often referred to as eddy covariance) method. Vertical transfer of heat and moisture in the atmosphere is significant when the atmosphere is turbulent, that is, when eddies in the wind carry heat and moisture up or down. Eddy correlation measures the up or down transfer of heat by using fast response temperature sensors that measure the instantaneous temperature and vertical wind speed differences from their means over a sampling period of about 30 min. The system makes multiple measurements each second, and computer processing calculates the correlation between vertical wind and temperature differences for determining heat flux, Q_H, and similarly between vertical wind and humidity for latent heat flux, Q_E.

To be accurate, these measurements must be made in the inertial sublayer above the roughness layer (Figs. 7.2 and 7.3), so that the measurements are not influenced by flow over individual surface elements. This generally requires that sensors be placed at least twice the height of the tallest buildings or trees, which generally excludes measurements over areas of "skyscraper" buildings. Also, because of the considerable effort and cost to operate a tower facility, there is seldom replication of the measurements for a particular land use in a city. The area sampled by an urban flux tower is usually up to about 2 km in radius, that is, at the local scale (see Table 7.1).

Researchers also make measurements of carbon dioxide (CO_2) from towers by eddy correlation. For example, measurements in a Baltimore, MD, suburb showed that while the area was a net source of CO_2 on an annual basis, the large amount of urban forest vegetation in the suburb created net uptake of CO_2 from the atmosphere during summer daytime hours [35]. Urban areas with little vegetation are net sources of CO_2 at all times.

7.5 Types of Urban Heat Islands

Because the magnitude and timing of the different types of urban heat islands and how they relate to urban built and vegetative structure differ greatly, it is important to distinguish between the different types (Table 7.3).

7.5.1 Urban Canopy Layer Heat Islands

In UHI studies, canopy layer air temperatures are usually measured at about the height of people or the lower stories of buildings, between 1.5 and 3 m above ground. If that temperature is warmer than the temperature at the same height in nearby rural areas, then this is termed an UCL heat island [37, 38]. This chapter focuses on urban canopy layer heat islands.

7.5.2 Urban Boundary Layer Heat Islands

The heat island that forms in the atmospheric boundary layer above the city is the urban boundary layer (UBL) heat island [29, 38]. As we have seen in Sect. 7.4.1, the UBL varies greatly in thickness and turbulence over the course of a clear day, and thus the UHI in the UBL also varies. During the night, if the sky is not heavily overcast, the UBL is only a shallow layer. During clear days, the mixed layer expands vertically. This process increases UBL thickness to 1 km or more [39]. Boundary layer heat islands are most often studied by using computer modeling at the mesoscale. A commonly noted feature in the modeling results is a plume extending downwind of a city [40].

A comparison of urban minus rural air temperature differences (Fig. 7.4) associated with the energy budget measurements in Fig. 7.1 suggests the difference between UCL and UBL heat islands. The graph shows hourly street-level urban-rural temperature differences, averaged over 30 days in midsummer, from measure-

Table 7.3 Simple classification scheme of urban heat island types [36]

UHI type	Location
Air temperature UHI	
Urban canopy layer heat island	Found beneath roof or treetop level
Urban boundary layer	Found above roof level; can be advected downwind with the urban plume
Surface temperature UHI	Different heat islands according to the definition of surface used (e.g., bird's eye view 2D vs. true 3D surface vs. ground)
Sub surface UHI	Found in the ground beneath the surface

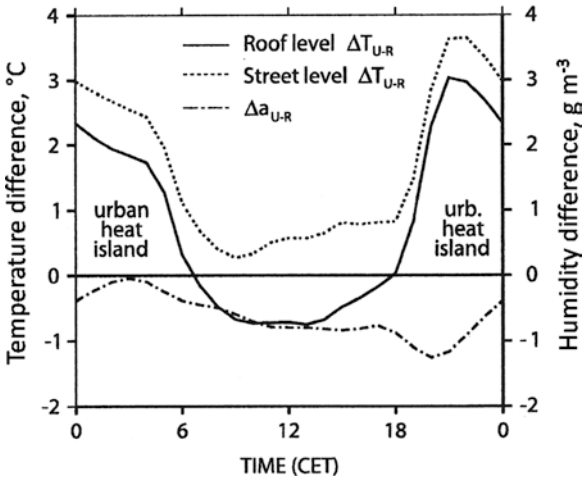

Fig. 7.4 Average urban-rural differences in air temperature (ΔT_{U-R}) at street level and above roof level, along with urban-rural absolute humidity differences (Δa_{U-R}) at sites where energy budget terms were measured above the urban and rural canopies as pictured in Fig. 7.1 [27]

ments at about 2.5 m above ground. It also shows the difference between temperatures at 5 m above the roofs (roof level) in a neighborhood of 10 m tall buildings compared to near ground-level rural temperatures. Both curves of ΔT_{U-R} show larger values at night, indicating the UHI effect. However, street-level ΔT_{U-R} UHI is larger and remains positive for all hours. Above roof level, ΔT_{U-R} is negative in midday because the vertical mixing in those hours brings relatively cool air from higher in the UBL down to the above roof level. Over all hours, the humidity difference, Δa_{U-R} in Fig. 7.4, was negative, which indicates greater humidity in rural areas. This is the result of greater evaporation in the rural agricultural area compared to the urban area with limited vegetation and available exposed soil.

7.5.3 Surface Urban Heat Islands (SUHI)

Urban heat islands may also be described by the temperatures of the upper surfaces of buildings, trees, streets, lawns, and so forth, as seen from above. This is sometimes called the urban "skin" temperature. This type of heat island should not be confused with "surface temperatures" as used in some climatology reports to refer to air temperatures near the ground, usually at a height of 1.5 m. The 1.5 m height is essentially *at* the surface of the Earth compared to the elevations at which temperatures are measured in atmospheric soundings (balloon measurements through the atmosphere), which may go to 30 km above the Earth. During the day, temperatures *of* the surfaces ("skin" temperatures) of nonliving solid material can be much warmer than air temperatures [41]. Temperatures of entire urban surfaces are generally measured by satellite [42]. With clear skies, upper surface heat islands are small at night and large during the day, the opposite of UCL air temperature heat islands [43].

Images of warm urban compared to rural skin temperatures as derived remotely from airplanes or satellites are commonly used as dramatic images of an UHI for the purposes of illustrating benefits of urban trees (e.g., [44]). Temperatures of trees and forests are usually not much above air temperature, and they can be shown in green in sharp contrast to a dark red for the commonly much warmer temperatures of building roofs and impervious asphalt surfaces. A benefit of such depictions is that the images show temperatures in a spatial continuum over a large area. However, the temperatures may be inaccurate because of the problem of correcting for absorption of thermal radiation through the atmosphere and for errors in apparent temperatures of surfaces that are not almost directly below the airplane or satellite and because the average emissivity ε of a large portion of a city is difficult to estimate.

7.5.4 Subsurface Urban Heat Islands

Though subsurface or soil urban heat islands have received less attention in research than air temperature or skin surface heat islands, soil temperatures are ecologically important. Soil temperatures control ecosystem processes such as release of CO_2 by respiration of fine-plant roots and soil microbes, nutrient cycling, nitrogen availability, and evaporation of water, which affects soil moisture. These multiple influences affect plant growth indirectly, and there are also direct effects of temperature on plant growth and storage of C in the soil [45]. Soil temperature also affects temperature of stormwater runoff, especially from impervious surfaces, and therefore stream temperatures are influenced (see Chap. 6) [46].

Very small-scale effects of surface cover or shading may affect near-surface soil temperatures much more than the UCL and UBL heat islands. Most studies of urban soil temperatures have concentrated on the effects of asphalt cover on temperatures of adjacent soil or of soil below the asphalt [25, 26]. However, a study in Baltimore, MD, analyzed average daily soil temperature at a 10 cm depth under turf grass and forest cover. Temperature was higher in urban than rural sites (15.0 °C vs. 13.5 °C) on an annual basis. Because of the moderating effects of forest cover, temperature differences were smaller in both urban forests[7] and rural forests than under turf grass, with annual averages being 12.6 °C for urban forest areas compared to 12.2 °C for rural forest areas [47].

7.6 Urban Heat Island Examples

Here we present some examples of UHI study results; some chosen from studies we have carried out. Other examples represent a range of methodologies. Most are studies of atmospheric UHI in the UCL. We justify presentation according to study

[7] Here "urban forest" refers to groups of closely spaced trees, such as wooded portions of parks within the city.

method because the method determines the spatial and temporal coverage of the conclusions.

7.6.1 Short-Term Temperature Measurements: Fixed Locations

Measurements near Baltimore, MD [48], illustrated the influence of land cover and land use on temperature differences (Fig. 7.5). Temperatures were measured at six suburban sites: a grassy area near a large apartment complex (apartments, Fig. 7.5a, c), a residential area with heavy tree cover but few buildings (residential under trees), a residential area with some trees and large lawn areas (residential open), a woodlot (wood), a large open pasture (rural open), and at the Baltimore/Washington International Airport (airport). The urban reference site was in downtown Baltimore (R in Fig. 7.5a); none of the suburban sites were far from some developed land uses (Fig. 7.5b). From May through September, average hourly temperature differences, ΔT, downtown site minus each of the other sites, were positive for all hours of the day. For most sites, ΔT through the day followed the usual UHI pattern of moist temperate climates—urban areas slightly warmer in midday, more rapid cooling of more rural areas after sunset leading to a maximum heat island in a few hours, and the cooler suburban areas heating more quickly after sunrise to approach the temperatures of urban areas that are heating more slowly. The wood site was coolest both day and night, and the other site with many trees, residential under trees, was similarly cool during the day. However, the residential under trees site was unusual in not cooling as much as other suburban sites at night, in part perhaps because of cold air drainage away from the site into a nearby valley (Fig. 7.5a, c).

7.6.2 Mobile Sampling

At least as early as the 1920s, mobile temperature sensing was used to study temperature differences across cities, and the method may be the one most used to derive urban heat island patterns [49–52]. Although usually limited in the number of days and time sampled, the mobile method offers a good way to sample across urban to rural gradients. Mobile transects are often used in combination with observations at fixed stations along the transect route and sometimes along with remote sensing to measure urban heat island patterns [53]. In Phoenix, AZ, automobile transects showed that during clear sky early mornings (beginning at 0500 h), industrial areas, which had the lowest vegetative cover, were warmest, commercial areas were just 1 °C cooler, residential and greenbelt were 3 °C cooler, and agricultural areas, which were irrigated, were 6 °C cooler. In summer afternoons, beginning at 1500 h, all land uses averaged within 2 °C of each other, with industrial being warmest and agriculture coolest [54].

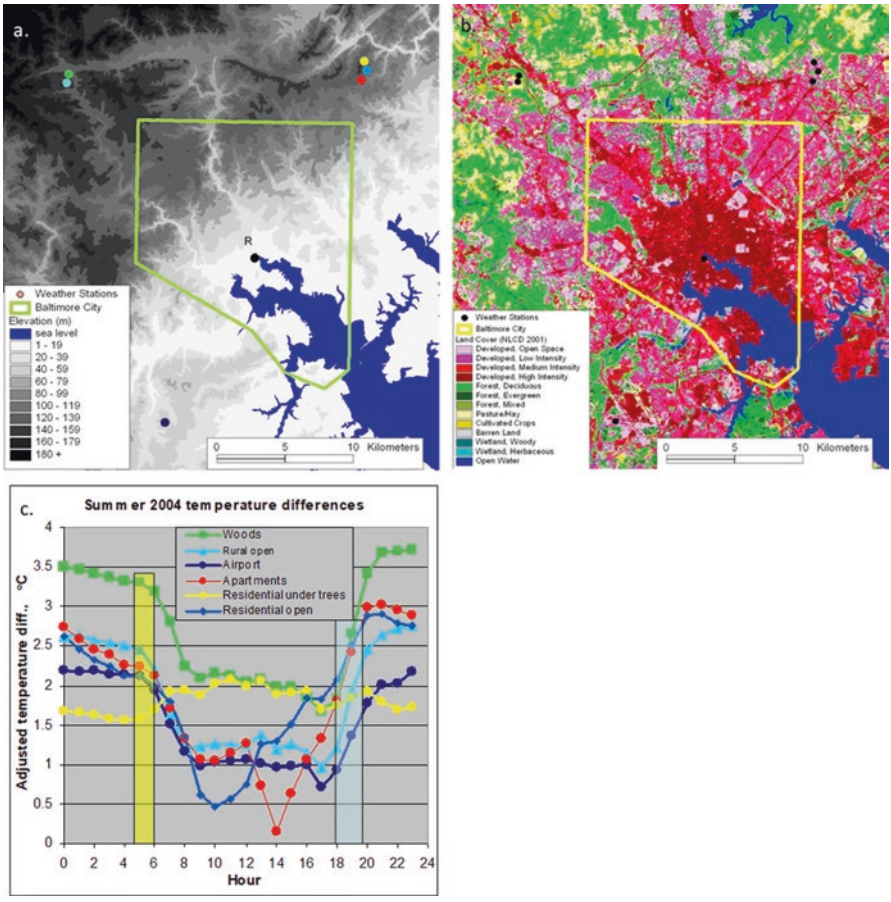

Fig. 7.5 (**a**) Elevation of Baltimore, MD, and vicinity with locations of 1.5-m-height temperature measuring sites color-coded to the average temperature differences in (**c**). (**b**) Land use for Baltimore and vicinity, with dark red being most developed, suburban residential mostly medium pink, developed open space such as parks light pink, agriculture yellow and brown, and forest green. (**c**) Differences in temperature, urban reference (*R*) minus other sites, averaged by hour of the day from May through September in different land-use categories. Temperatures adjusted for elevation difference. Range of times of sunrise and sunset indicated by shaded yellow and blue

In winter, the Phoenix measurements showed smaller temperature ranges: only 2 °C in the morning and only 1 °C in the afternoon. Measurements in some other cities have also shown smaller UHIs in winter, but others have shown winter UHIs to be greater than summer UHIs. It seems that the difference in magnitude of UHIs between summer and winter is sufficiently small that careful analysis is needed to assess which season has the most intense UHI. The difference between summer and winter UHIs depends largely upon the winter versus summer temperatures and solar radiation climate, which determine the amount of energy used for heating and cooling buildings.

In Puerto Rico, results from automobile measurements showed that the San Juan UHI has reached outward from the center of the city toward the east about 25 km [53]. In this case, the transect followed a main highway along which there was considerable recent development.

7.6.3 Analysis of Long-Term Records

Long-term temperature records can show the influence of urbanization, especially where temperature records are available from the start of development. A rare example of where this was possible was for Columbia, Maryland, where, in 1968, just after the start of the development, a heat island effect of 1 °C was observed in a small residential area, and a 3 °C heat island was found in a large parking lot. Six years later, the population had reached 20,000, and the maximum UHI had increased to 7 °C [1].

Analysis of historical data (GHCN, see Box 7.3) provided a comparison of UHI trends during the twentieth century for Baltimore, MD, and Phoenix, AZ [23]. The useable climate records began as early as 1908 and extended to 1997 for some stations. For the Baltimore region, the analysis used average daily maximum and minimum temperatures for July. For Phoenix, data were from May. Time series of the urban-minus-rural temperatures ($\Delta T\max_{U-R}$) at the time of the daily maximum temperature showed a difference between the humid, forested Baltimore compared to the arid desert Phoenix. In Baltimore, urban maximums are usually warmer than rural, whereas in the Phoenix area, urban maximum temperatures tend to be cooler than rural maximums (Fig. 7.6a, b). That is, values of $\Delta T\max_{U-R}$, which occur in daytime, tend to be negative in Phoenix, making an urban cool island. We believe this results partly from extensive watering of plants in urban areas, though the high rate of warming at the rural desert reference stations may be another part of the cause [55]. In both Baltimore and Phoenix, there are only slight long-term trends of changing $\Delta T\max_{U-R}$. Thus, evaluation of a city's overall UHI requires inclusion of nighttime observation.

Box 7.3: Historical Climate Data (GHCN)
One source of long-term records is the Global Historical Climate Network (GHCN) maintained by the National Centers for Environmental Information (NCEI) of the US National Oceanic and Atmospheric Administration (NOAA). The GHCN databases are available for public access online (search GHCN). The databases include quality-assured daily and monthly climate summaries from land surface stations across the Earth. For some stations many variables are provided, including temperature, total daily precipitation, snowfall, and snow depth; however, about two-thirds of the stations report just precipitation. Length of records varies from station to station, but for some, data extend to over 175 years.

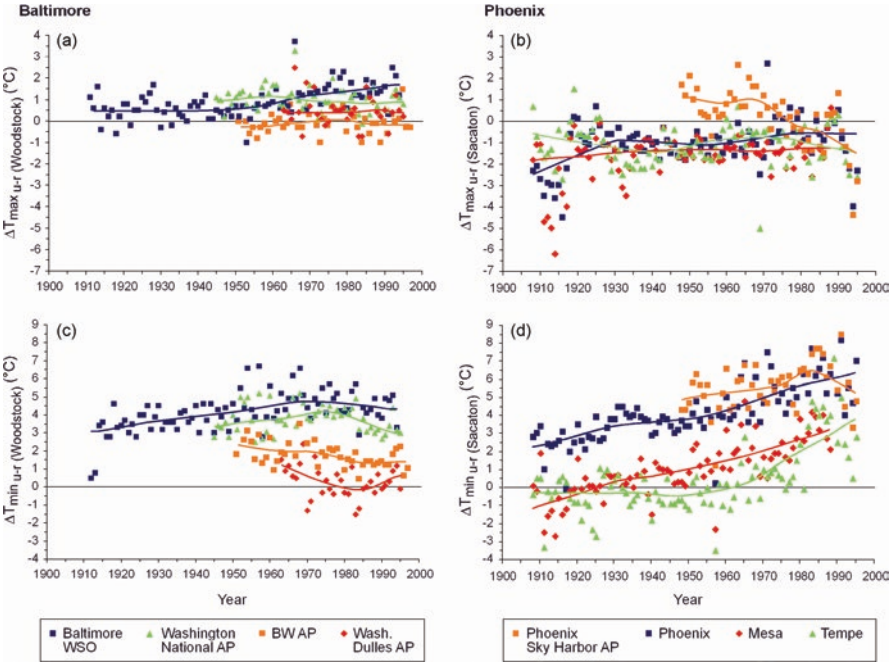

Fig. 7.6 (**a**) Long-term July monthly averages of maximum daily urban temperature minus corresponding rural temperatures (at Woodstock, MD about 24 km west of Baltimore) for stations in and near Baltimore. (**b**) May monthly maximum daily urban temperature minus rural temperatures (at Sacaton, AZ south of Phoenix) for the Phoenix region, and (**c**) and (**d**) monthly averages of minimum daily urban temperatures minus corresponding rural temperatures. From Brazel et al. [23]

There were definite long-term trends in urban-minus-rural temperature ($\Delta T\text{min}_{U-R}$) at the time of the daily minimum temperature (Fig. 7.6c, d). The $\Delta T\text{min}_{U-R}$ values tend to reflect population trends in the two cities. In Baltimore, $\Delta T\text{min}_{U-R}$ peaked at 4.5 °C in 1970, and decreased slightly after that, apparently because of population declines within the city and development encroaching on the rural site. In Phoenix, $\Delta T\text{min}_{U-R}$ increased substantially from about 2.5 °C in 1908, when population was only a few thousand to 6.5 °C in 1995 when population was about 700,000. As is typical of most cities, the UHI increase with population was rapid in early years of development and then increased at a slower rate as the city grew large. The rural comparison site for Phoenix, Sacaton, developed little during the twentieth century.

Thus, as has been found in many other cities, the UHI in both Baltimore and Phoenix is primarily manifested in increased nighttime temperatures rather than in greatly increased temperatures during the warmest part of the day. Many other cities show a long-term warming trend that can be attributed to both increasing urban heat island effect as population increases and to global climate change (see Sect. 7.10).

Another pertinent comparison of the heat island in different cities is the maximum intensity of the urban heat island, $\Delta T_{U-R(\max)}$, which is similar to $\Delta T\text{min}_{U-R}$,

which usually occurs at night. Average $\Delta T_{U-R(\max)}$ has been found to vary with population [56] as we saw for $\Delta T\min_{U-R}$ in Baltimore and Phoenix. Because of the different typical city structure, $\Delta T_{U-R(\max)}$ is usually greater in the United States than in European cities of equal population. Tropical and subtropical cities have generally smaller $\Delta T_{U-R(\max)}$ values than higher-latitude cities [57]. Also, $\Delta T_{U-R(\max)}$ tends to be lower in wet than dry climate tropical and subtropical cities.

7.6.4 Empirical Modeling

To evaluate the influence of urban cover on UCL air temperatures, especially the influence of urban trees on temperature, a study of Baltimore, MD, used regression analysis with high-resolution (10 m) remotely sensed tree and impervious cover data along with hourly weather data to develop relationships for predicting temperature differences (ΔT) between the reference site (indicated by "R" in Fig. 7.5a) in central Baltimore and the six other weather stations in different land uses around the city [21]. One predictor of ΔT was the difference in upwind land cover between stations. Land cover had an influence on air temperature, but there were strong interactions between land cover and other predictors of ΔT, particularly atmospheric stability and topography. Land cover differences out to 5 km in the upwind direction were significantly related to ΔT under stable atmospheric conditions (Turner Class stability index, see Box 7.1, was a useful indicator of urban heat island intensity).

The regression equations combined with recent GIS tools [58] permitted mapping ΔT across a mesoscale-sized area of Baltimore and surroundings (Fig. 7.7). The GIS methods have the potential for testing the effects on temperature of changed land cover, for example, by inputting and mapping different scenarios of altered tree or impervious cover. Figure 7.7a is for midafternoon of a partly cloudy summer day with low wind speeds, which created moderately unstable conditions (Turner Class 2, see Box 7.1). The coolest point is 4.1 °C cooler than the warmest. But more than half of the predicted temperature difference is due to differences in elevation. With the elevation factor removed from the ΔT prediction equation (Fig. 7.7b), the influences of land cover alone are illustrated for the same time as in Fig. 7.7a; land cover causes a ΔT range of about 1.6 °C. In Fig. 7.7c, with clear sky and low wind speed at night (Turner Class 7, very stable), the UHI effect is near maximum. A large city park (Patterson) is about 2 °C cooler than the dense residential area surrounding it. The patterns of elevation and land use are evident in the pattern of predicted ΔT in Fig. 7.7c.

7.6.5 Mesoscale Meteorological Models

Mesoscale meteorology models are used to carry out numerical simulations of atmospheric conditions over three-dimensional atmospheric space with horizontal extent of up to thousands of kilometers and vertical extent of the entire lower

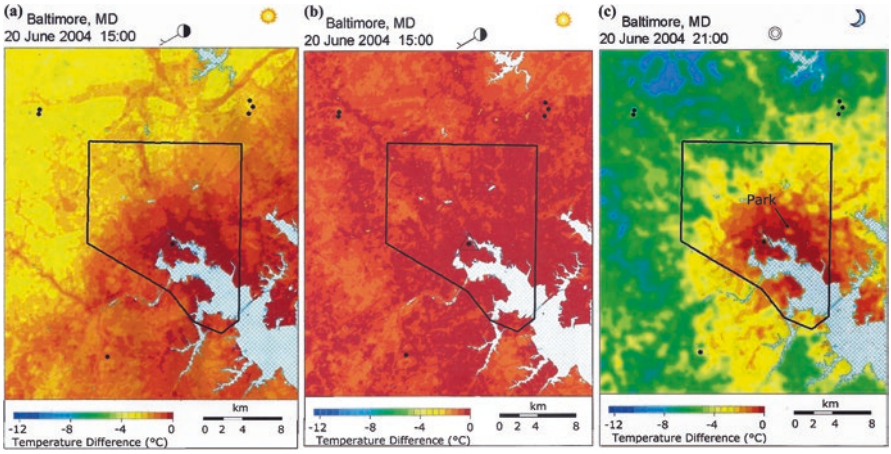

Fig. 7.7 (**a**) Modeled air temperature differences (ΔT) at 1.5-m-height across Baltimore, (black line) and vicinity. Black dots indicate weather stations. This map is for 1500 local standard time of a partly cloudy summer day with low wind speeds (<2.6 m/s = 5 kt), Turner stability Class 2. Water shown by cross-hatched blue. Solid colors indicate ΔT with respect to the warmest temperature on the map (dark red). The coolest point (light yellow) is 4.1 °C cooler. (**b**) With the elevation factor removed from the ΔT equation, the influences of land cover are illustrated for the same time as in (**a**); land cover causes a ΔT range of about 1.6 °C. (**c**) With clear sky and low wind speed at night, Turner Class 7, the UHI effect is near maximum. A large city park (Patterson) is about 2 °C cooler than the dense residential area surrounding it. See Fig. 7.8a for elevation map of the Baltimore area and Fig. 7.8b for land use

atmosphere. They are used in a wide range of studies and disciplines, such as weather prediction, hydrologic modeling, air chemistry, atmospheric dispersion, regional and climate assessments, and urban climate. The models simulate meteorological conditions, such as wind, temperature, and vertical mixing. They may be used for predicting air temperature near the ground (2 m in height), wind speed and direction at 10 m above ground (the international standard height for wind measurements), and air quality, including ozone and fine particle concentrations.

Mesoscale model development has been underway for more than three decades and has progressed as computer capabilities have progressed to be able to carry out the solutions of huge numbers of primitive (based on first principles) equations that begin with those describing the conservation of mass, heat, and motion [60]. Mesoscale modeling today most often uses the Weather Research and Forecasting (WRF) model, a numerical weather prediction system that serves both forecasting and atmospheric research needs. Mesoscale models couple the ground surface to the atmosphere, and they require ground cover conditions as input. Varying horizontal scales may be used; for modeling city-scale processes, the grid spacing is less than with synoptic scale models, but still large, typically about 2 km, though in some cases as small as 0.5 km [61].

A mesoscale study with 0.5 km resolution evaluated the afternoon UHI in the Baltimore-to-Washington metropolitan area [62]. The UHI patterns for Baltimore derived by the mesoscale modeling were similar in general form to the UHI pattern

using the empirical method described in Sect. 7.6.4; and the magnitudes of the UHI were similar, 4–5 °C, by both methods. The 10 m resolution of the empirical data produced much more detail in the UHI pattern, detail that would be useful for planning UHI mitigation such as by tree planting [21]. The mesoscale maps covered not just Baltimore and near vicinity but also the entire area from Baltimore to Washington. This led to the conclusion that the PBL plume from Washington, DC, may have enhanced the magnitude of the UHI in Baltimore UCL by 1.25 °C [62].

7.7 Urban Wind

Modifications to wind flow by buildings and trees strongly interact with air temperature, radiation balances, and heat storage terms to affect urban climate, human comfort and health, and energy use in buildings. Although our emphasis in this chapter is on urban structure influences on air temperature, the environmental influence of trees and buildings on wind speed and turbulence will often be greater than influences on temperature.

7.7.1 Effects of Trees and Buildings on Wind

A study in relatively low-building-density residential neighborhoods in Pennsylvania measured wind speed at the 2 m height in four neighborhoods of single-family detached houses that were selected for their similar housing stock and different tree cover [63]. The mostly deciduous tree cover ranged from near 0% to 77%, and building footprints within the neighborhoods ranged from 6% to 12% of the area. Measurements at houses were adjusted for the effect of the houses at which the measurements were made. That is, the purpose of the study was to determine the effective wind force on individual houses, but when wind speed is measured just upwind of a building, the building itself will reduce wind speed; the adjustment increased apparent wind speed accordingly. Apparent wind reductions by other houses throughout the neighborhoods ranged from 21% to 24%, and by trees from 28% to 46% in summer and 14% to 41% in winter (Fig. 7.8). Thus, with the loss of leaves in winter, wind reductions by trees were 50% less in the low-tree-density neighborhood, but only 5% and 11% less in the neighborhoods with greater tree cover.

In the Pennsylvania analysis, average wind speed reduction in summer as a percentage, U_r, was approximately related to the sum of tree canopy and building footprint cover as a percentage, $C_{b,t}$, by

$$U_r = 100C_{b,t} / \left(24 + 1.1C_{b,t}\right). \tag{7.6}$$

When tree and building cover are relatively low, a small increase in density has a large effect in reducing wind speed (Fig. 7.9).

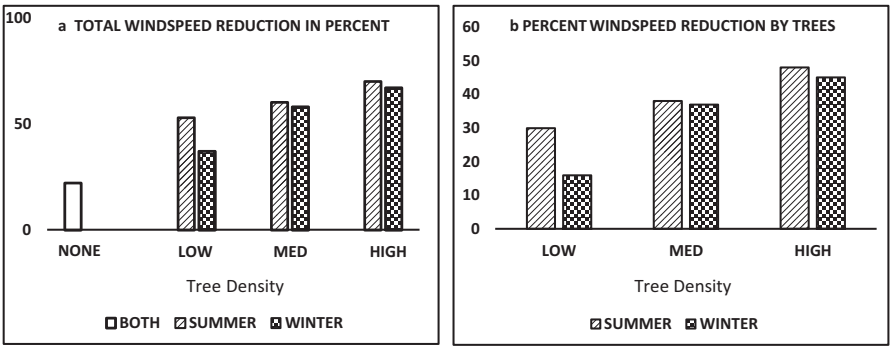

Fig. 7.8 (**a**) Mean wind speed reductions and (**b**) apparent reductions by trees in four neighborhoods, with different tree density [63]

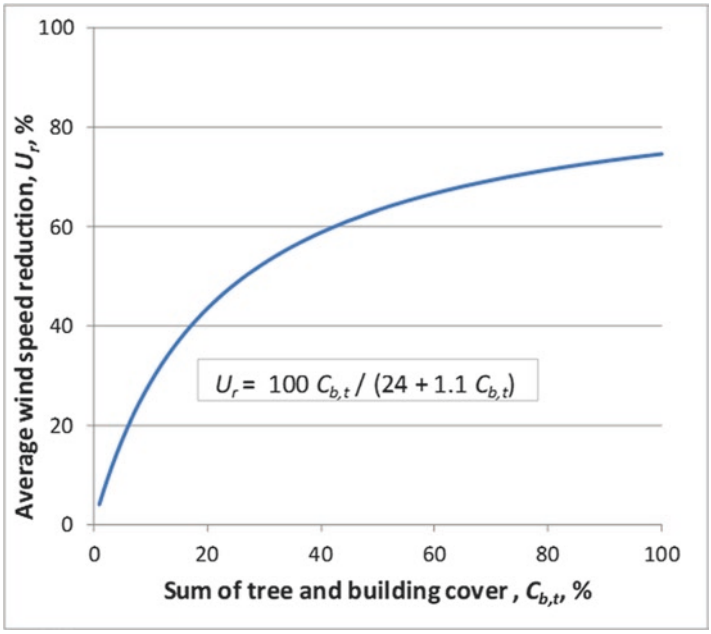

Fig. 7.9 Average wind speed reduction in summer by trees and buildings in neighborhoods of single-family detached houses in Central Pennsylvania [63]

Tall buildings in cities, especially where some skyscraper-type buildings are much taller than others, create complex flow at ground level. Wind perpendicular and at a high elevation on a tall building wall may be directed down the face of the building and then accelerated around the corners of the building. Near pedestrian level, wind may be increased to two or three times the speed of wind in an area with

no buildings [64]. On the downwind side of tall buildings, there tends to be an area of reduced wind speed, but direction may be opposite to that of the undisturbed flow.

In an area of Dayton, Ohio, with scattered tall buildings, wind speed increased with height of the nearest upwind building and decreased with distance from the building, evidently an effect of acceleration around the corners of buildings [65]. The measurements in Dayton were carried out with regional thermal stability ranging from neutral to moderately unstable. Relative wind speed (wind in city/wind at airport) increased with decreasing stability. Unstable conditions increase turbulence in wind flow. The decreasing effect of obstacles to reduce mean wind speed as stability decreases is similar to the effect observed in many studies of tree-row windbreaks that show reduced effectiveness with increased turbulence of the wind approaching the windbreak [66]. Even in the Dayton central business district, street trees significantly decreased wind speed [67].

7.7.2 UHI-Driven Air Flow

A city will generate its own local country-to-city wind regime due to the heat island effect when regional winds are very light [8]. Warm, unstable air in the city rises, creating a low-pressure area that induces air to move from the country to converge and rise in the city center. When regional winds are exceptionally low, the city thermal winds may exceed wind speed in the country [68].

The UHI effect may also impact more regional topographically induced thermal wind systems. The center of Phoenix, AZ, lies on a relative flat area with a long gradual slope up toward mountains on the northeast. Mesoscale modeling showed that during the afternoon, regional winds tend to blow upslope and up smaller valleys toward the mountains. At night, there tends to be cool air drainage downslope toward the city. The modeling showed that (a) between 1973 and 2005, local winds in the city area were increasingly slowed by the rapid growth of the city and (b) the urban area slowed the upslope winds flowing away from the city to the north and east during the day [61]. Thus, not only did the urban area impact overall wind speed but also imposed differential effects on the prevailing topographic thermally driven wind system.

7.7.3 Sea Breeze in Cities

Cities located on coasts of large lakes and near oceans experience yet another diurnal wind system that we know as the sea breeze (land breeze at night). This phenomenon is driven again by differential heating, in this case of land and water, with the result of onshore flow during the day (cooler air off the water toward the heated land) and offshore flow at night. There are myriad examples in urban climate of the importance of these breezes for human comfort (especially for tropical cities), air

quality, and the dimension of the UHI. Usually sea breezes bring cooler air from the water to seaside cities. This is the case with the massive UHI of the city of Tokyo that observations showed may be moderated by up to about 2 °C, with some cooling extending for at least 10 km into the city [69, 70].

In the case of Hong Kong, a large tropical city on hilly topography surrounded by irregular ocean coastline on three sides, ventilation by air movement at pedestrian height is a key factor in ameliorating the large UHI that develops in that city. Rather than creating ventilation that would reduce the UHI, the complex topography with up- or downslope winds and sea breeze combine under some synoptic wind flow conditions to produce air stagnation and dangerously high air pollution levels [71, 72]. Hong Kong has water on the east, west, and south. Under light synoptic winds from the north, the sea breezes from the other three directions converge to cause the air stagnation. The dense, total building landscape of Hong Kong exacerbates the lack of adequate ventilation. In some cases, large blocks are entirely covered by one building just a few stories tall, a "podium," upon which tall skyscrapers stand. A podium greatly reduces air movement at pedestrian height. Much effort has been expended for planning to incorporate ideas important for future design of the city [73].

7.8 Urban Effects on Precipitation

Much research has been carried out on the proposition that urban areas significantly affect precipitation [74]. Cities may affect precipitation in a variety of ways: by increasing *convection*[8] through the UHI effect, by high levels of pollutants that form *cloud condensation nuclei (CCN)*, and by the increase in roughness and upward forcing of air flow over areas of tall buildings [1]. Other possible urban influences on precipitation are diverting of storm systems around cities and by irrigated urban areas in dry climates serving as sources of moisture needed for convective development [74]. The small or negative daytime heat island in Phoenix, which exists because of irrigation, has consequences for urban convection effects on precipitation. The convection probably is greater just outside the urban core than within it. However, examination of long-term precipitation trends for the Phoenix area suggests a 12–14% increase of rainfall in the generally downwind direction from the city center [75].

METROMEX was a large multi-year research project with the primary goal of investigating the effects of St. Louis on precipitation [76]. Four years of research indicated that St. Louis increased summer rainfall downwind of the urban-industrial complex [77], and the increases amounted to as much as 45% [1]. The increase appeared to be caused by intensification of natural storm systems by a combination of the UHI and by addition of condensation nuclei from pollution. Lightning, which is caused by the vertical convection process, was also significantly increased in St. Louis, primarily downwind of the city center [78].

[8] This convection consists of the vertical rise of air that has been heated and thus made buoyant by the urban area.

One reason that uncertainties remain about urban influences on precipitation is the considerable natural spatial variation of storm totals from point to point. Equally problematic is the difficulty of accurately measuring precipitation with rain gauges. The main types of errors are (1) those caused by positioning of the gauge so that precipitation is shielded from the opening of the gauge; (2) by wind diverting the rain and, especially, snow from the opening; and (3) errors of the measuring system within the gauge. Most commonly used rain gauges today are of the tipping bucket type, which have two small bins, or "buckets" that alternate catching the rain until full and then tip, dumping their catch and making an electrical contact to provide a count. Accurate measurement of precipitation is sufficiently important for water management in many cities around the world that researchers have expended considerable effort to derive methods to calibrate and correct rain gauge errors [79].

7.9 Influences of Parks

Parks in urban areas not only serve recreational functions but create their own microclimatic conditions, which especially for large cities in warm climates provide a cooling ecosystem service for the public. Although the prevailing idea is that parks cool an area [80], the magnitude and even the direction (+ or – relative to its surroundings) of the impact of a park on temperature within an urban area depend on a host of factors such as shape, size, composition (% trees, grass, water, impervious ground, and density of vegetation), and kind of land cover surrounding the park. Table 7.4 gives some examples of park nighttime cooling impacts, size of parks, and "extension" distances of cooling effects away from the park that have been detected. There appears to be no clear pattern to the park effects. Generally, it is assumed that bigger parks would affect larger surrounding areas, but this is not always the case, as the composition and roughness of surrounding areas partially dictate this impact. Another subtle effect is the tree canopy impacts at night. A heavily tree-covered park may be warmer than a park with large grass areas, because outgoing LW radiation to a cold night sky may be larger than in a tree-covered area [81]. Fig. 7.7c points to a large city park in Baltimore that empirical modeling predicted will be about 2 °C cooler than surrounding areas at 9:00 PM. There are seven other large parks in Baltimore that had easily recognized influences on temperature. The parks averaged 1.7 °C to 5.9 °C cooler than the warmest location in the city at 9:00 PM on a clear night with low wind speed [90].

7.10 Relationship to Global Climate Change

The UHI effect in even modest-sized cities is at times much larger than the approximately 1.0 °C of average global temperature warming above preindustrial levels estimated to have been caused by human activities by the Intergovernmental Panel on Climate Change [82]. This is true especially on clear nights with low wind

Table 7.4 Maximum temperature difference (Max. ΔT_{u-p} °C) from surrounding city and extent of park influences on temperature at a range of latitudes and climate types [80]

City	Latitude, °N	Climate	Park size (ha)	Max. ΔT_{u-p} °C	Extension (*m*)
Washington, DC	40	Humid subtropical	–	3–5	
Mexico City	20	Short grass prairie	525	6	2000
München	48	Humid continental	130	3.5	
			2.5	2.0	
Montreal	45	Humid continental	38	2.0	400
Kumamoto city	33	Humid continental	2.25	4	20
			0.24	3	15
Kuala Lumpur	3	Tropical rain forest	153	4.1	
			46	3.1	
			19	1.9	
			1.6	1.5	
Goteborg	57	Marine west coast	156	6	1500
Tucson	32	Hot dry desert	171	6.8	

speeds. Global warming is caused by accumulation of "greenhouse" gases (GHG) in the stratosphere, a completely different phenomenon than the processes that cause UHIs. However, global warming and UHI effects are linked because a large portion of the GHGs are produced in urban areas and the UHI effect modifies, either positively or negatively, the urban emissions of GHGs [5]. Positive UHI contributions to GHG come from increased energy use for air conditioning in summer. Negative contributions may come from reduced energy use for heating buildings in winter, though this effect is generally not considered. Perhaps more importantly, the UHI effect makes terrestrial air temperature monitoring of the global effect uncertain because for many weather stations it is difficult to separate UHI influences from the global influences [83, 84].

7.11 Mitigation of Urban Heat Islands

When considering the literature on the mitigation of urban heat islands, special attention should be paid to experimental design, assumptions of the study, and the language. Ask yourself if experimenters were without bias in designing the experiment and interpreting results, or whether they consciously or unconsciously set out to show the benefits of their method of heat island mitigation. When a research team is charged with the responsibility to propose UHI mitigation strategies, it is difficult to avoid being overly optimistic about possible effects of the proposed strategies.

Studies of UHI mitigation are most often limited in some way. Studies in temperate climates usually consider only summer and not winter. Thus, possible winter

benefits of UHI are often not considered. The most common approaches to UHI reduction are increasing albedo of urban surfaces, or "whitening," and large-scale tree planting [85]. A study to predict the effects on mitigation of the UHI of New York City if tree planting, white pavements and roofs, and green roofs were implemented used mesoscale modeling and satellite skin surface images to predict "near-surface" air temperatures [86]. The study concluded that all of the mitigation strategies could reduce summer UHIs, but the best was a combination of tree planting (on 17.5% of city area) and living roofs, which had the potential of reducing peak afternoon temperatures by 0.7 °C if fully implemented. Any possible negative influences by reductions of winter air temperature or increases in heating costs for buildings by tree shade were not considered, and possible net benefits of trees and living roofs in winter were also not considered.

Another mesoscale modeling study for a large city predicted that the Los Angeles, CA, heat island could be reduced by as much as 3 °C by "cooler" (lighter) roof and paving surfaces and the planting of 11 million more shade trees [87]. The most common application of whitening has been for roofs, though light-colored paving has also been recommended [88]. A similar study predicted that increasing the albedo of streets and of residential, commercial, and industrial areas in the Los Angeles basin from 0.139 to 0.155 would reduce predicted 1500 h air temperatures by 2 °C, which would cause a significant reduction in predicted ozone concentrations [89].

Another mitigation effect could be the use of irrigation of vegetation. In Phoenix, a small cool island exists during the day, apparently because of irrigation of vegetation in the city [23, 61]. In Los Angeles, the maximum air temperatures decreased during the city's early development, as dry arid regions were replaced with irrigated orchards and farmland [88].

The US Environmental Protection Agency tried over many years to produce for planners and administrators a set of scientific explanations for UHI effects and guidelines for mitigation of UHIs on which most researchers in the field could generally agree. The current online version (as of 2008 and 2009) covers in separate documents: UHI basics, mitigation by trees and other vegetation, green (living) roofs, cool (light colored) roofs, cool pavements, and activism in the cause of UHI reduction including tree planting programs, ordinances, and building codes and zoning [90]. The US EPA has this and a wide range of other applied information on their website titled "Heat Island Effect."

7.12 Conclusions

The feature of urban climate systems that is usually of most concern is that urban areas usually have warmer air temperatures than more rural areas, the urban heat island effect, UHI. The magnitude of the UHI generally increases with city size and population. The UHI is usually not more than 3 or 4 °C during midday. Depending upon the rural reference site and synoptic weather conditions, the UHI effect in large cities may range up to about 11 °C, usually within a few hours after sunset (see Sect. 7.6).

Comparisons of urban to nonurban climate are seldom made between urban conditions and those representative of conditions before development. The comparison is usually with agricultural areas, where the environment has already been drastically modified by humans. Dry, desert climates have maximum UHIs of similar magnitude to moist climates, unless the rural comparison is with unirrigated desert. In that case, during the daytime, the temperature island may turn out to be a small-magnitude cool island, in part because of evaporative cooling of irrigated vegetation within the city and because the dry desert becomes very warm owing to the low admittance of desert vegetation and soils (Sects. 7.3.3 and 7.6.3.).

Urban heat islands are caused by a combination of factors:

- The high thermal admittance (high thermal entropy) of urban building and infrastructure materials that lead to greater daytime storage and nighttime release of heat in urban than rural areas (Sect. 7.3.4)
- Less vegetation and availability of soil moisture in urban areas that lead to less evapotranspiration and a larger proportion of net radiation (commonly termed Q^* in climate literature) going into sensible heat flux (Q_H) than latent heat flux (Q_E) in urban areas (Sect. 7.3.3)
- Emissions of heat from buildings, transportation facilities, and industrial processes (Sect. 7.3.1)
- Greater air pollution and aerosols in urban areas, which usually leads to an increase in Q^* (Sect. 7.3.2)
- The effect of tall buildings in trapping thermal radiation within canyon-like building walls, thus effectively increasing the overall urban Q^* and reducing nighttime cooling by outgoing thermal radiation (Sect. 7.3.2)
- The effect of tall buildings in reducing mixing of near-surface air with cooler air at higher elevations (Sect. 7.7.1)

The UHI effect is usually considered to be detrimental. Warmer temperatures increase ozone production in urban atmospheres; increase use of energy for air conditioning, thereby increasing emissions of CO_2; and increase adverse effects on human health and mortality in heat waves. In temperate climates, UHIs are usually greater in summer than winter because of the greater amount of solar insolation in summer. However, substantial UHIs can also form in winter, with the benefits of reducing costs for heating buildings and less snow and ice hazard. The winter benefits of UHIs have seldom been quantified and compared to the detriments of summer (Sect. 7.11).

The most common approaches to UHI reduction are increasing vegetation cover and increasing albedo of urban surfaces, or "whitening." Urban whitening most often takes the form of making roof surfaces lighter so that solar radiation is reflected back to space, effectively reducing Q^* in the urban energy budget. Increasing vegetation includes "green roofs," which insulate roofs and increase evapotranspiration causing greater Q_E, and tree planting, which shades high thermal admittance surfaces and also increases Q_E (Sect. 7.11.)

Urban areas have effects on precipitation and wind that are partly the result of warming due to an UHI. The precipitation effect usually results in increases down-

wind of the city center. The UHI effect on wind generally occurs with very light synoptic winds when air rises over the warm city to cause low level flow into the city. Trees throughout residential areas with low building density may have dramatic effects on wind speed with reductions of over 40% even in winter where most trees are deciduous (Sects. 7.7 and 7.8).

Global climate change and the UHI effect are caused by completely different physical processes, the global change in temperature caused by changes in upper atmosphere constituents, and the UHI effect by land cover. However, the UHI effect makes air temperature monitoring of the long-term global climate change uncertain because many weather stations are influenced by urban influences (Sect. 7.10).

Acknowledgments The first author thanks the many students and technical support staff who assisted with research on urban forest climate influences, including Karla Hyde, Yingjie Wang, David Murphy, Greg Bacon, Michelle Bunny, Andrew Lee, Emma Noonan, and Hang Ryeol Na. GIS maps were prepared by Alexis Ellis. The Baltimore Ecosystem Study LTER, operating with contributions from the National Science Foundation grant DEB 0423476, provided some of the instrumentation and technical support staff. This chapter was improved by suggestions on an earlier draft from Nancy Selover, Arizona State Climatologist; Ian Yesilonis, Soil Scientist, USDA Forest Service; and Jacqueline Lu, Director of GIS and Analytics, NYC Parks.

References

1. Landsberg HE (1981) The urban climate. Academic, New York
2. Grimm NB, Faeth SH, Golubiewski NE, Redman CL, Wu J, Bai X, Briggs JM (2008) Global change and the ecology of cities. Science 319:756–760
3. Oke TR (1997) Urban climates and global environmental change. In: Thompson RD, Perry A (eds) Applied climatology: principles and practice. Routledge, London, pp 273–287
4. Sanchez-Rodriguez R, Seto KC, Simon D, Solecki WD, Kraas F, Laumann G (2005) Science plan: urbanization and global environmental change. International Human Dimensions Programme on Global Environmental Change, Bonn
5. Mills G (2007) Cities as agents of global change. Int J Climatol 27:1849–1857. https://doi.org/10.1002/joc.1604
6. Mills G (2006) Progress toward sustainable settlements: a role for urban climatology. Theor Appl Climatol 84:69–76
7. Karl TR, Jones PD (1989) Urban bias in area-averaged surface air temperature trends. Bull Am Meteorol Soc 70:265–270
8. Oke TR (1987) Boundary layer climates. Methuen, London
9. Akbari H, Pomerantz M, Taha H (2001) Cool surfaces and shade trees to reduce energy use and improve air quality in urban areas. Sol Energy 70:295–310. https://doi.org/10.1016/S0038-092x(00)00089-X
10. Brazel AJ, Crewe K (2002) Preliminary test of a surface heat island model (SHIM) and implications for a desert urban environment, Phoenix, Arizona. J Ariz Nev Acad Sci 34:98–105
11. Gates DM (1980) Biophysical ecology. Springer, New York
12. Brown RD, Gillespie TJ (1995) Microclimatic landscape design: creating thermal comfort and energy efficiency. Wiley, New York
13. Grimmond CSB, Oke TR (1995) Comparison of heat fluxes from summertime observations in the suburbs of four North American cities. J Appl Meteorol 34:873–889

14. Sailor DJ (2011) A review of methods for estimating anthropogenic heat and moisture emissions in the urban environment. Int J Climatol 31:189–199
15. Fan H, Sailor DJ (2005) Modeling the impacts of anthropogenic heating on the urban climate of Philadelphia: a comparison of implementations in two PBL schemes. Atmos Environ 39:73–84
16. Heisler GM, Grant RH (2000) Ultraviolet radiation in urban ecosystems with consideration of effects on human health. Urban Ecosyst 4:193–229
17. Gomes L, Roger JC, Dubuisson P (2008) Effects of the physical and optical properties of urban aerosols measured during the CAPITOUL summer campaign on the local direct radiative forcing. Meteorog Atmos Phys 102:289–306
18. Brazel AJ, Quatrocchi D (2005) Urban Climatology. In: Oliver J (ed) Encyclopedia of world climatology. Springer, New York, pp 766–779
19. Yap D (1975) Seasonal excess urban energy and the nocturnal heat island—Toronto. Arch Meteorol Geophys Bioklimatol Ser B 23:69–80
20. Voogt JA, Oke TR (1997) Complete urban surface temperatures. J Appl Meteorol 36:1117–1132
21. Heisler GM, Ellis A, Nowak DJ, Yesilonis I (2016) Modeling and imaging land-cover influences on air temperature in and near Baltimore, MD. Theor Appl Climatol 124:497–515. https://doi.org/10.1007/s00704-015-1416-z
22. Kaye MW, Brazel A, Netzband M, Katti M (2003) Perspectives on a decade of climate in the CAP LTER region. Central Arizona - phoenix long-term ecological research (CAP LTER). http://caplter.asu.edu/docs/symposia/symp2003/Kaye_et_al.pdf
23. Brazel A, Selover N, Vose R, Heisler GM (2000) The tale of two climates -- Baltimore and Phoenix urban LTER sites. Clim Res 15:123–135
24. Kalanda BD, Oke TR, Spittlehouse DL (1980) Suburban energy balance estimates for Vancouver, B.C. using the Bowen ratio-energy balance approach. J Appl Meteorol 19:791–802
25. Halverson HG, Heisler GM (1981) Soil temperatures under urban trees and asphalt. USDA, Northeastern Forest Experiment Station, Broomall
26. Celestian SB, Martin CA (2004) Rhizophere, surface, and air temperature patterns at parking lots in Phoenix, Arizona, U.S. J Arboricult 30:245–252
27. Christen A, Vogt R (2004) Energy and radiation balance of a Central European city. Int J Climatol 24:1395–1421
28. Piringer M et al (2002) Investigating the surface energy balance in urban areas -- recent advances and future needs. Water Air Soil Pollut Focus 2:1–16
29. Oke T, Mills G, Christen A, Voogt J (2017) Urban Climates. Cambridge University Press, Cambridge. https://doi.org/10.1017/9781139016476
30. Oke TR (2006) Initial guidance to obtain representative meteorological observations at urban sites. World Meteorological Organization, Geneva
31. Panofsky HA, Dutton JA (1984) Atmospheric turbulence. Wiley, New York
32. Comrie A (2000) Mapping a wind-modified urban heat island in Tucson, Arizona (with comments on integrating research and undergraduate learning). Bull Am Meteorol Soc 81:2417–2431
33. Brazel AJ, Fernando HJS, Hunt JCR, Selover N, Hedquist BC, Pardyjak E (2005) Evening transition observations in Phoenix, Arizona. J Appl Meteorol 44:99–112
34. Pielke RAS et al (2007) Unresolved issues with the assessment of multidecadal global land surface temperature trends. J Geophys Res 112:D24S08. https://doi.org/10.1029/2006JD008229
35. Crawford B, Grimmond CSB, Christen A (2011) Five years of carbon dioxide fluxes measurements in a highly vegetated suburban area. Atmos Environ 45:896–905
36. Oke TR (2006) Towards better communication in urban climate. Theor Appl Climatol 84:179–189
37. Oke TR (1976) The distinction between canopy and boundary-layer urban heat islands. Atmos 14:268–277
38. Oke TR (1995) The heat island of the urban boundary layer: characteristics, causes and effects. In: Cermak JE, Davenport AG, Plate EJ, Viegas DX (eds) Wind climate in cities. Kluwer Academic Publishers, Dordrecht, pp 81–107

39. Stull RB (2000) Meteorology for scientists and engineers (second edition). Brooks/Cole, Pacific Grove
40. Krayenhoff ES, Martilli A, Bass B, Stull RB (2003) Mesoscale simulation of urban heat mitigation strategies in Toronto, CA. In: Fifth international conference on urban climate, Lodz, Poland, September 1–5 2003. International Association for Urban Climate (IAUC)
41. Hartz DA, Prashad L, Hedquist BC, Golden J, Brazel AJ (2006) Linking satellite images and hand-held infrared thermography to observed neighborhood climate conditions. Remote Sens Environ 104:190–200
42. Gallo KP, McNab AL, Karl TR, Brown JF, Hood JJ, Tarpley JD (1993) The use of a vegetation index for assessment of the urban heat island effect. Int J Remote Sens 14:2223–2230
43. Voogt JA, Oke TR (2003) Thermal remote sensing of urban climates. Remote Sens Environ 86:370–384
44. Moll G, Berish C (1996) Atlanta's changing environment. Am For 102:26–29
45. Shaver G et al (2000) Global warming and terrestrial ecosystems: a conceptual framework for analysis. Bioscience 50:871–882
46. Pouyat RV, Belt K, Pataki D, Groffman PM, Hom J, Band L (2007) Urban land-use change effects on biogeochemical cycles. In: Jea C (ed) Terrestrial ecosystems in a changing world. Global change: the IGBP series. Springer, Berlin, pp 45–58
47. Savva Y, Szlavecz K, Pouyat RV, Groffman PM, Heisler G (2010) Effects of land use and vegetation cover on soil temperature in an urban ecosystem. Soil Sci Soc Am J 74:469–480
48. Heisler G et al (2006) Land-cover influences on air temperatures in and near Baltimore, MD. In: 6th international conference on urban climate, Gothenburg, Sweden. International Association for Urban Climate [Available online http://www.gvc2.gu.se/icuc6//index.htm], pp 392–395
49. Hart MA, Sailor DJ (2009) Quantifying the influence of land-use and surface characteristics on spatial variability in the urban heat island. Theor Appl Climatol 95:317–406. https://doi.org/10.1007/s00704-008-0017-5
50. Hedquist B, Brazel AJ (2006) Urban, residential, and rural climate comparisons from mobile transects and fixed stations: Phoenix, Arizona. J Ariz Nev Acad Sci 38:77–87
51. Stabler L, Martin CA, Brazel A (2005) Microclimates in a desert city were related to land use and vegetation index. Urban For Urban Green 3:137–147
52. Sun C-Y, Brazel A, Chow WTL, Hedquist BC, Prashad L (2009) Desert heat island study in winter by mobile transect and remote sensing techniques. Theor Appl Climatol 98:323–335
53. Murphy DJ, Hall MH, Hall CAS, Heisler GM, Stehman SV, Anselmi-Molina C (2011) The relationship between land cover and the urban heat island in northeastern Puerto Rico. Int J Climatol 31:1222–1239. https://doi.org/10.1002/joc.2145
54. Martin CA, Stabler LB, Brazel AJ (2000) Summer and winter patterns of air temperature and humidity under calm conditions in relation to urban land use. In: Third symposium on the urban environment. Davis, CA. 14–18 August, 2000. American Meteorological Society, Boston, pp 197–198
55. Georgescu M, Moustaoui M, Mahalov A, Dudhia J (2011) An alternative explanation of the semiarid urban area "oasis effect". J Geophys Res 116:D24113. https://doi.org/10.1029/2011JD016720
56. Oke TR (1973) City size and the urban heat island. Atmos Environ 7:769–779
57. Roth M (2007) Review of urban climate research in (sub)tropical regions. Int J Climatol 27:1859–1973
58. Ellis A (2009) Analyzing canopy cover effects on urban temperatures. M.S. Thesis, SUNY College of Environmental Science and Forestry, Syracuse. Available from http://gradworks.umi.com/14/82/1482101.html
59. Nowak DJ, Heisler GM (2010) Air quality effects of urban trees and parks. National Recreation and Parks Association Research Series Monograph, Ashburn. p 44. https://www.fs.fed.us/nrs/pubs/jrnl/2010/nrs_2010_nowak_002.pdf

60. Pielke RA Sr (2002) Mesoscale meteorological modeling, International geophysics series, vol 78. Academic, San Diego
61. Grossman-Clarke S, Zehnder JA, Loridan T, Grimmond CSB (2010) Contribution of land use changes to near-surface air temperatures during recent summer extreme heat events in the Phoenix metropolitan area. J Appl Meteorol Climatol 49:1649–1664
62. Zhang D-L, Shou Y-X, Dickerson RR, Chen F (2011) Impact of upstream urbanization on the urban heat island effects along the Washington–Baltimore corridor. J Appl Meteorol Climatol 50:2012–2029
63. Heisler GM (1990) Mean wind speed below building height in residential neighborhoods with different tree densities. ASHRAE Trans 96:1389–1396
64. Penwarden AD, Wise AFE (1975) Wind environment around buildings. Building Research Establishment, Department of the Environment, London
65. Grant RH, Heisler G, Herrington LP, Smith D (1985) Urban winds: the influence of city morphology on pedestrian level winds. In: Seventh conference on biometeorology and aerobiology, Scottsdale, Arizona. American Meteorological Society, pp 353–356
66. Heisler GM, DeWalle DR (1988) Effects of windbreak structure on wind flow. Agric Ecosyst Environ 22/23:41–69
67. Heisler GM (1987) Grant RH predicting pedestrian-level winds in cities. In: Preprint volume of the 18th conference agricultural and forest meteorology and 8th conference biometeorology and aerobiology. American Meteorological Society, pp 356–359
68. Lee DO (1979) The influence of atmospheric stability and the urban heat island on urban-rural wind speed differences. Atmos Environ 13:1175–1180
69. Ashie Y, Konob T (2011) Urban-scale CFD analysis in support of a climate-sensitive design for the Tokyo Bay area. Int J Climatol 31:174–188
70. Oda R, Kanda M (2009) Cooling effect of sea surface temperature of Tokyo Bay on urban air temperature. In: The seventh International Conference on Urban Climate, Yokohama, Japan, 29 June to 3 July. http://www.ide.titech.ac.jp/~icuc7/extended_abstracts/pdf/375843-1-090518085335-004.pdf
71. Liu HP, Chan JCL (2002) Boundary layer dynamics associated with a severe air-pollution episode in Hong Kong. Atmos Environ 36:2013–2025
72. Lo JCF, Lau AKH, Chen F, Fung JCH, Leung KKM (2007) Urban modification in a mesoscale model and the effects on the local circulation in the Pearl River Delta Region. J Appl Meteorol Climatol 46:457–476
73. Ng E, Cheng V (2006) Air ventilation assessment system for high density planning and design. IAUC Newsl 19:11–13
74. Shepherd JM (2005) A review of current investigations of urban-induced rainfall and recommendations for the future. Earth Interact 9:1–27
75. Shepherd JM (2006) Evidence of urban-induced precipitation variability in arid climate regimes. J Arid Environ 67:607–628
76. Braham RR, Jr (1977) Overview of urban climate. In: Heisler GM, Herrington LP (eds) Proceedings of the conference on metropolitan physical environment. USDA Forest Service, Syracuse, pp 3–25. Available at http://www.treesearch.fs.fed.us/pubs/24033
77. Huff FA (1977) Mesoscale features of urban rainfall enhancement. In: Heisler GM, Herrington LP (eds) Proceedings of the conference on metropolitan physical environment, vol. general technical report NE-25. USDA Forest Service, Northeastern Forest Experiment Station, Upper Darby, pp 18–25. http://www.treesearch.fs.fed.us/pubs/24033
78. Shepherd JM, Stallins JA, Jin ML, Mote TL (2010) Urbanization: impacts on clouds, precipitation, and lightning. In: Aitkenhead-Peterson J, Volder A (eds) Urban ecosystem ecology. Agronomy monograph, 55th edn. American Society of Agronomy, Crop Science Society of America, Soil Science Society of America, Madison
79. Molini A, Lanza LG, La Barbera P (2005) The impact of tipping-bucket raingauge measurement errors on design rainfall for urban-scale applications. Hydrol Process 19:1073–1088

80. Upmanis H, Eliasson I, Lindqvist S (1998) The influence of green areas on nocturnal temperatures in a high latitude city (Göteborg, Sweden). Int J Climatol 18:681–700
81. Herrington LP, Bertolin GE, Leonard RE (1972) Microclimate of a suburban park. In: Conference on urban environment and second conference on biometeorology. American Meteorological Society, Philadelphia, pp 43–44
82. Intergovernmental Panel on Climate Change (2018) Summary for policy makers (SPM), IPCC SR1.5
83. Christy JR, Goodridge JD (1995) Precision global temperatures from satellites and urban warming effects of non-satellite data. Atmos Environ 29:1957–1961
84. Kalnay E, Cai M (2003) Impact of urbanization and land-use change on climate. Nature 423:528–531
85. Gartland L (2008) Heat Islands, understanding and mitigating heat in urban areas. Earthscan, London
86. Rosenzweig C, Solecki WD, Slosberg RB (2006) Mitigating New York city's heat island with urban forestry, living roofs, and light surfaces. Columbia University Center for Climate Systems Research & NASA/Goddard Institute for Space Studies, New York
87. Rosenfeld AH, Akbari H, Romm JJ, Pomerantz M (1998) Cool communities: strategies for heat island mitigation and smog reduction. Energ Buildings 28:51–62
88. Rosenfeld AH, Akbari H, Bretz S, Fishman BL, Kurn DM, Sailor D, Taha H (1995) Mitigation of urban heat islands: materials, utility programs, updates. Energ Buildings 22:255–265
89. Taha H, Douglas S, Haney J (1997) Mesoscale meteorological and air quality impacts of increased urban albedo and vegetation. Energ Buildings 25(2):169–177
90. Environmental Protection Agency (2008) Reducing urban heat islands: compendium of strategies. http://www.epa.gov/heatislands/resources/compendium.htm. Accessed 3 June 2011